Downstream structures of interplanetary fast shocks associated with coronal mass ejections

R. Kataoka, S. Watari, N. Shimada, H. Shimazu, and K. Marubashi

National Institute of Information and Communications Technology, Tokyo, Japan

Received 21 February 2005; revised 12 May 2005; accepted 20 May 2005; published 18 June 2005.

[1] We investigate 17 coronal mass ejection (CME) events identified by the ACE spacecraft during solar cycle 23, focusing upon the fine structures of the sheath region between the CME and its associated shock to find their dependence on the shock parameters. We observe the planar magnetic structure (PMS) downstream of a quasi-perpendicular shock when the Alfvén Mach number >2.0. Here, the PMS is characterized by the magnetic fields changing directions abruptly and intermittently within a plane parallel to the shock plane. The downstream PMS does not form when a magnetic cloud with β value <0.05 exists just upstream of a shock with Alfvén Mach number <2.0. The sheath magnetic fields become highly turbulent when the shock angle is <60 and/or the upstream β value is >0.5 and the upstream is dominated by Alfvenic fluctuations. **Citation:** Kataoka, R., S. Watari, N. Shimada, H. Shimazu, and K. Marubashi (2005), Downstream structures of interplanetary fast shocks associated with coronal mass ejections, *Geophys. Res. Lett.*, *32*, L12103, doi:10.1029/2005GL022777.

1. Introduction

[2] When an interplanetary fast shock forms ahead of an interplanetary coronal mass ejection (ICME), the compressed region bounded by the shock front and the ICME leading edge is referred to as the sheath. The fine structure of the sheath region is an important research target of the present space weather study for possible roles of; driving great geomagnetic storms [*Tsurutani et al.*, 1988], impeding the propagation of energetic particles [*Sanderson et al.*, 2000], and a precursor indicating geometries of oncoming ICMEs [*Jones et al.*, 2002]. It is a challenging issue to predict the fine structure of the sheath region because the sheath field sometimes appears to be turbulent without ordered structures.

[3] An interesting feature found in the sheath region is the planar magnetic structure (PMS) that is characterized by the magnetic fields having a series of abrupt changes in directions parallel to a single plane due to directional discontinuities (DDs) [*Nakagawa et al.*, 1989]. The formation of the PMS by the draping of the interplanetary magnetic field (IMF) around the ICME was suggested by *Farrugia et al.* [1990]. Extending the draping hypothesis, *Neugebauer et al.* [1993] suggested that the associated interplanetary fast shocks cause the amplification and alignment of preexisting discontinuities in the ambient solar wind to produce the PMS.

0094-8276/05/2005GL022777

[4] The draping hypothesis was supported by the consistent orientation of the PMS with respect to the large-scale ICME structure [*Jones et al.*, 2002]. However, important problems still remain unsolved, e.g., the relationship between orientations of the PMS and the shock plane, the preferable upstream condition for the formation of the downstream PMS, and the relationship between the PMS and the turbulent IMF. Using the solar wind data obtained from ACE (Advanced Composition Explorer) placed in a halo orbit around the L1 point, we investigate the downstream structures of 17 interplanetary fast shocks associated with ICMEs, focusing on the shock parameter dependences of the PMS formation in the sheath region.

2. Event Selection

[5] In this paper, the first criterion of an ICME event is a coexistence of a maximum solar wind speed >600 km/s and a maximum magnetic field strength >20 nT during a 24 hour interval. Secondly, we eliminate the cases corresponding to the corotating stream that is identified by a stream interface followed by relatively high temperatures and low densities. Finally, we adopt a criterion for the identification of an ICME event itself, that at least two of the following four conditions must be satisfied during the 24 hour interval; the ratio of proton thermal pressure to magnetic pressure <0.1, proton temperature less than a half of the empirical temperature derived as a function of the solar wind speed [*Lopez*, 1987], density ratio of α particles to protons >0.1, and an existence of bidirectional streaming electrons [*Gosling et al.*, 1987].

[6] Using the above criteria, a total of 35 ICME events are identified for the period from February 1998 to October 2004. Interplanetary fast shocks are clearly found in 27 of the 35 ICME events. We eliminate three shock events in which multiple shocks exist within 12 hours, because such events are caused by multiple halo CMEs and the shock upstream and/or downstream are highly contaminated by some merged solar wind structures. Since our analyses shown below require the ACE Level 2 data of 16 sec magnetic fields and 64 sec plasma parameters, unavailability of the Level 2 data further eliminates seven more shock events. As a result, the full set of our analyses is applied to a total of 17 shock events.

[7] Figure 1 shows a schematic representation of a typical shock event. Magnetic fields are provided in the geocentric solar ecliptic (GSE) polar coordinate system; θ is the colatitude measured from the Z axis and φ is the longitude measured from the X axis, pointing toward the Sun. Interplanetary fast shocks are identified by abrupt enhancements in the magnetic field strength B, solar wind speed V,

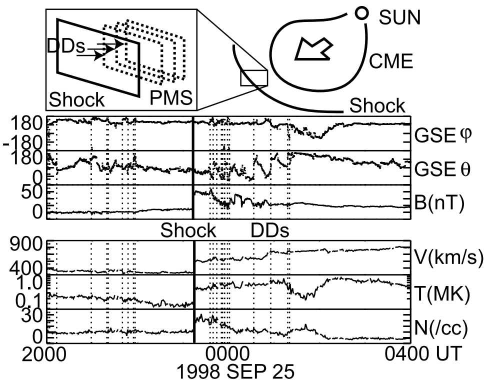

Figure 1. A schematic representation of the PMS in the sheath region with an actual data example. Top and bottom three panels show the ACE 16 sec magnetic field and 64 sec plasma data for an 8 hour interval. Directional discontinuities are indicated by dotted lines.

proton temperature T, and proton density N. The large-amplitude IMF disturbances are found downstream of the shock. This is the sheath region, where the solar wind speed and temperature are higher than average. Dotted lines in Figure 1 show the occurrences of DDs. In this paper, the criterion of the DDs is >60° rotation of the IMF direction within 128 sec. This is a severe criterion for DDs. However, the results shown below do not change essentially, even if we use more moderate criteria.

3. Shock Analysis

[8] Characteristics of the interplanetary fast shocks are indicated by three upstream conditions; the shock angle θ_{Bn}, the Alfvén Mach number $M_A = V_n/V_A$, and the β value. Here θ_{Bn} is the acute angle between the shock normal and magnetic field, V_n the upstream speed in the normal incidence frame, V_A the Alfvén speed, and β the ratio of the proton thermal pressure to the magnetic pressure. It is worthwhile noting here that we use V_A instead of $V_A \cos\theta_{Bn}$ for the estimation of M_A because the shock parameter dependence of the PMS formation becomes simple.

[9] The coplanarity theorem is used to derive the shock normal. We calculate the shock normal of Abraham-Shrauner method [*Abraham-Shrauner and Yun*, 1976], following the pre-averaged method as introduced in detail by *Berdichevsky et al.* [2000]. The estimated shock normal is further validated from arrival times of the shock at any available spacecraft in the interplanetary medium. As a result, the potential error of the normal direction is estimated to be at most 15°.

4. Downstream Structures

[10] Figures 2, 3, and 4 show the scatter plots of IMF directions during the 2 hour intervals just upstream (blue circles) and downstream (red circles) of the shocks in the GSE polar coordinate system. The 2 hour period is selected because the sheath region continues at least 2 hours for all of the 17 events. Shock normal directions and the shock planes are indicated by crosses and solid lines, respectively. In order to evaluate the existence of the PMS in the downstream, first we evaluate the planarity using the

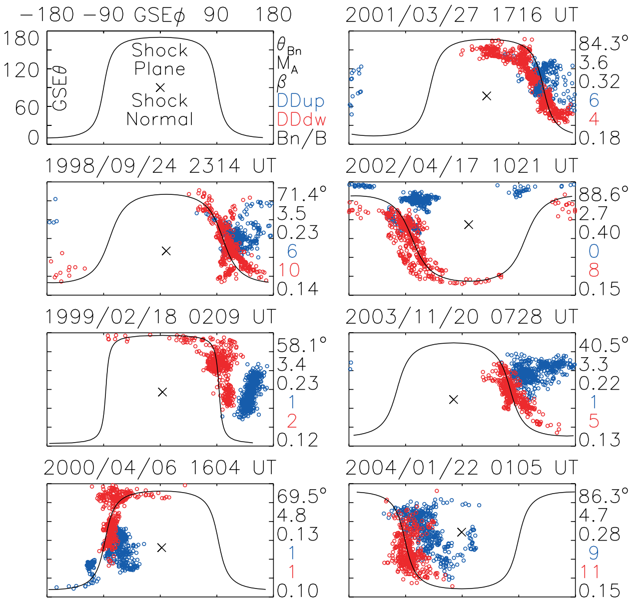

Figure 2. Scatter plots of magnetic field directions in the GSE polar coordinate system during 2 hour intervals upstream (blue circles) and downstream (red circles) of the interplanetary fast shocks. Downstream PMS events with Bn/B < 0.2 are shown. Shown at the top of each panel is the arrival time of the interplanetary shock at the ACE spacecraft. Shock normal directions and the shock planes are indicated by crosses and solid lines, respectively. From top to bottom of the right side of each panel, shown are the shock parameters θ_{Bn}, M_A, and β, occurrence numbers of DDs upstream and downstream, and the value of Bn/B.

magnetic field projection on the direction of the shock normal. The projected magnetic field Bn is normalized by the total magnetic field strength B. The averaged values of the Bn/B during the 2 hours are shown on the lower right side of each panel in Figures 2, 3, and 4.

[11] We categorize the 17 shock events into three groups, which are separately shown in Figures 2, 3, and 4. Figure 2

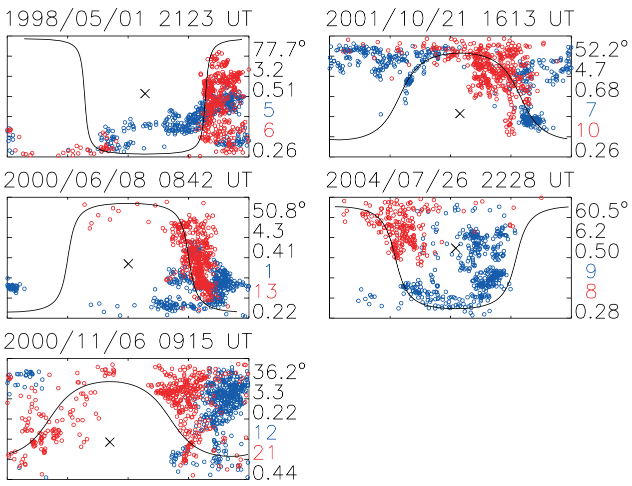

Figure 3. Scatter plots of upstream and downstream IMF directions for the turbulent downstream events with Bn/B > 0.2. The format is the same as Figure 2.

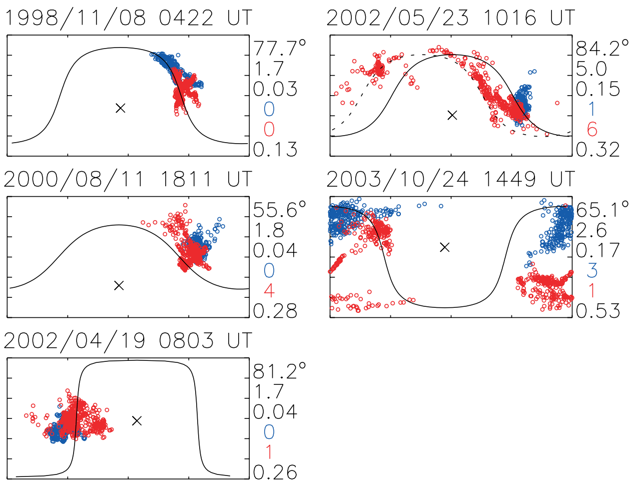

Figure 4. Scatter plots of upstream and downstream IMF directions for the events with some exceptional features as explained in the text. The format is the same as Figure 2.

shows the 7 shock events with an excellent planarity as indicated by the small downstream value of Bn/B (i.e., Bn/B < 0.2). The upstream IMF directions distribute around the Parker spiral direction that is the φ angle of $-45°$ or $135°$. The downstream IMF directions are scattered in both θ and φ directions following the shock plane directions. Except for one event, the shock angle θ_{Bn} tends to be large, indicating a quasi-perpendicular shock. Figure 3 shows the 5 shock events with a poor planarity as indicated by the large value of Bn/B > 0.2. The upstream IMF directions themselves are rather disordered and deflected from the Parker spiral direction. The downstream IMF directions are also scattered in both θ and φ directions poorly following the shock plane directions. This group is characterized by the shock parameters of high upstream β values (>0.5) and/or small shock angle θ_{Bn} (<60°). Figure 4 shows the remaining 5 shock events which have some exceptional features in the scatter plots. The shock effects on the scattering and alignment of the IMF directions are less evident in the weak shock events with M_A < 2.0 as shown in the left column. Two other events in the right column, which are strong quasi-perpendicular shock cases, have large values of Bn/B > 0.2 even though the shock parameters are similar to those of the events in Figure 2.

[12] PMS-like structure is indicated not only by small values of Bn/B but also by an existence of DDs. DDs cause the spread in orientations of the magnetic field downstream and upstream of the shock as shown in Figures 2, 3, and 4. The numbers of DDs during the 2 hour intervals upstream and downstream of the shock are indicated as DDup and DDdw, respectively. Downstream DDs exist in all of the events except for the November 1998 event. In our study, upstream DDs were not observed within two hours ahead of a weak shock event, as shown in the left column of Figure 4. Figure 5a shows a scatter plot of DDup and DDdw, where the shock events in Figures 2, 3, and 4 are indicated by open circles, solid circles, and crosses, respectively. It is found that DDdw is comparable with or larger than DDup. Note that the November 2000 event has 12 and 21 DDs in the upstream and downstream, respectively, which is out of the plot range in Figure 5a to enlarge the main distribution.

[13] The turbulent and large amplitude fluctuations in the solar wind are known as Alfvénic fluctuations [*Belcher and Davis*, 1971], and the turbulence is sometimes evaluated by the Alfvénicity. In this paper, the Alfvénicity index is defined as the three-component correlation coefficients [cf. *Marubashi*, 1996] between magnetic field **B** and velocity vectors **V**,

$$A = \pm\frac{1}{n}\sum_{i=0}^{n-1}\frac{\mathbf{B}(i)-\overline{\mathbf{B}}}{\sqrt{\frac{1}{n}\sum_{j=0}^{n-1}\left(\mathbf{B}(j)-\overline{\mathbf{B}}\right)^2}}\cdot\frac{\mathbf{V}(i)-\overline{\mathbf{V}}}{\sqrt{\frac{1}{n}\sum_{j=0}^{n-1}\left(\mathbf{V}(j)-\overline{\mathbf{V}}\right)^2}}, \quad (1)$$

where n is the sample number of the vectors, and the bar means the average. The positive/negative sign in the right hand side of the equation (1) is taken when the spacecraft locates in the toward/away IMF sector, in order to define that the ideal Alfvén waves propagating outward and inward are indicated by $A = 1$ and -1, respectively.

[14] Using 64 sec values of magnetic field and velocity data with $n = 30$, the time interval for the evaluation of the Alfvénicity index is 32 min in this study. The results shown below do not change essentially, even if we take longer time interval for this analysis. Figure 5b shows a scatter plot of the maximum Alfvénicity indices Aup and Adw obtained within the 2 hour intervals upstream and downstream, respectively. The positive values >0.6 obtained in all of the events indicate a characteristic of outward propagating Alfvén waves. It is also found that the upstream Alfvénicity is strongly positive >0.95 in the shock events in Figure 3, while it tends to be reduced downstream. This means that outward propagating Alfvén waves are particularly enhanced in the upstream of these events, and that the Alfvénic fluctuations tend to develop into turbulences after crossing the shock.

5. Discussions

[15] As shown in Section 4, we find that the downstream PMS formation depends on the shock parameters as follows: the PMS is generated downstream of a strong shock with M_A > 2.0 and the IMF in the PMS region is directed mostly perpendicular to the shock normal as shown in Figure 2; the PMS is not observed when the M_A is <2.0 and the upstream β value is <0.05 as shown in the left column of Figure 4; and the IMF directions are deflected from the shock plane directions when the shock angle is <60° and/or the upstream β value is >0.5 as shown in

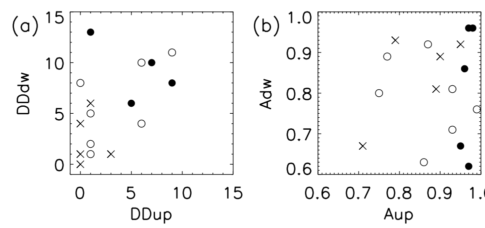

Figure 5. Scatter plots of (a) the numbers of DDs and (b) the Alfvénicity indices in the upstream and downstream. Open circles, solid circles, and crosses indicate the shock events in Figures 2, 3, and 4, respectively.

Figure 3. It is worthwhile noting here that, inversely speaking, the knowledge of the shock parameter dependence of the downstream PMS helps to gain confidence on the accuracy of the evaluated shock normal. We discuss the physical meanings of the obtained shock parameter dependences in association with the inherent properties of the solar wind plasma.

[16] As shown in Figure 5a, the occurrence rate of downstream DDs is comparable with or larger than that of upstream DDs. This result is consistent with the suggestion that interplanetary fast shocks may cause the amplification and alignment of preexisting DDs in the ambient solar wind to produce the PMS [e.g., *Neugebauer et al.*, 1993]. Larger number of downstream DDs is also consistent with the results from hybrid simulations that the interaction between a shock and a discontinuity can produce multiple discontinuities in the downstream [e.g., *Lin et al.*, 1996].

[17] The lack of upstream DDs themselves in the weak shock events in the left column of Figure 4 is due to the fact that a possible magnetic cloud structure exists just in front of the shock and that the trailing edge of the magnetic cloud is compressed by the shock. Magnetic clouds are characterized by extremely low temperatures and strong magnetic fields with smooth rotations of the directions [*Burlaga et al.*, 1981], causing extremely low β values and the absence of DDs. The low β condition further causes a local Alfvén speed higher than average and M_A smaller than average. As a result, the compression rate at the shock is smaller than average. Therefore, because of the plasma properties of magnetic clouds, these events have neither upstream DDs nor strong compressions at the shock, which are necessary conditions for the PMS formation by the shock propagation.

[18] In the events shown in Figure 3, when the shock angle is small and/or the upstream β value is high, IMF directions during 2 hour upstream are rather disordered and deflected from the Parker spiral direction. Figure 5b shows that the upstream solar wind is the highly Alfvénic stream where the Alfvénicity index is >0.95. It is expected that an interplanetary fast shock experiences a highly variable θ_{Bn} during the shock passage of such a solar wind structure. This high variability may be an essential cause of the relatively strong magnetic fields parallel to the shock normal, which remain in the downstream. It is worthwhile noting here that the quasi-parallel shock itself would not be a sufficient condition to produce the parallel fields remained in the downstream because an excellent PMS is observed in the quasi-parallel shock event on November 20, 2003 as shown in Figure 2.

[19] Finally, we discuss the other two exceptional events in the right column of Figure 4. In the May 2002 event, a significant difference is found between the shock plane and the PMS alignment. The dotted line shows the 45° shift of the shock normal in the negative φ direction. A possible interpretation is that the PMS is strongly affected by the draping process in this event, as suggested by *Jones et al.* [2002]. If the PMS is affected strongly by the draping around an ICME, the PMS should be aligned to the ICME front rather than the shock plane. The difference between the orientations of ICME front and shock plane should be significant when the spacecraft passed through the very edge of the ICME.

[20] Additional ACE data also support this interpretation. In this event, the magnetic cloud following the sheath region has a smooth but quite small rotation of the IMF directions with enhanced Bx component, suggesting the spacecraft passage of the very edge of the flux rope structure. Further, the solar wind flow is extremely deflected from the Sun-Earth line in the sheath region, which is an expected signature of the draped field. What we can learn from this example is that the PMS orientation would be controlled not only by the shock plane but also by the ICME front, and such a draping effect can be evident in a special geometry. Using multiple spacecraft, an analogous situation in the terrestrial context was investigated in detail by *Farrugia et al.* [1991].

[21] In the October 2003 event in the right column of Figure 4, a smooth rotation of the IMF directions starts at 30 min after the shock arrival from (90°, −150°) to (50°, 150°) in the (θ, φ) coordinates, during over 30 min. The IMF directions in this region are different from the shock plane directions. This phenomenon looks like a mini flux rope structure embedded within the sheath region, although the proton temperature during this period is as high as surrounding sheath region. What we can learn from this example is that such merged solar wind structure can disturb the PMS.

6. Conclusion

[22] The shock parameter dependence is found for the formation of the PMS in the ICME sheath region. Strong ($M_A > 2.0$) and quasi-perpendicular ($\theta_{Bn} > 60°$) shocks are the most preferable conditions for the PMS formation. The shock parameter dependence is also associated with the inherent upstream plasma properties of the solar wind, such as low-β magnetic clouds and high-β Alfvénic streams.

[23] **Acknowledgments.** We thank the ACE MAG and SWEPAM instrument team and the ACE Science Center for providing the ACE data. R. K. is supported by a research fellowship of the Japan Society for the Promotion of Science for Young Scientists.

References

Abraham-Shrauner, B., and S. H. Yun (1976), Interplanetary shocks seen by AMES plasma probe on Pioneer 6 and 7, *J. Geophys. Res.*, *81*, 2097.

Belcher, J. W., and L. Davis (1971), Large-amplitude Alfvén waves in the interplanetary medium, 2, *J. Geophys. Res.*, *76*, 3534.

Berdichevsky, D. B., et al. (2000), Interplanetary fast shocks and associated drivers observed through 23rd solar minimum by Wind over its first 2.5 years, *J. Geophys. Res.*, *105*, 27,289.

Burlaga, L. F., et al. (1981), Magnetic loop behind an interplanetary shock: Voyager, Helios and IMP-8 observations, *J. Geophys. Res.*, *86*, 6673.

Farrugia, C. J., et al. (1990), An interplanetary planar magnetic structure oriented at a large (~80 deg) angle to the Parker spiral, *Geophys. Res. Lett.*, *17*, 1025.

Farrugia, C. J., et al. (1991), Multipoint observations of planar interplanetary field structures, *J. Atmos. Terr. Phys.*, *53*, 1039.

Gosling, J. T., et al. (1987), Bidirectional solar wind electron heat flux events, *J. Geophys. Res.*, *92*, 8519.

Jones, G. H., et al. (2002), The draping of heliospheric magnetic fields upstream of coronal mass ejecta, *Geophys. Res. Lett.*, *29*(11), 1520, doi:10.1029/2001GL014110.

Lin, Y., et al. (1996), Generation of dynamic pressure pulses downstream of the bow shock by variations in the interplanetary magnetic field orientation, *J. Geophys. Res.*, *101*, 479.

Lopez, R. (1987), Solar cycle invariance in solar wind proton temperature relationships, *J. Geophys. Res.*, *92*, 11,189.

Marubashi, K. (1996), Corotating and transient structures of the interplanetary magnetic fields at Venus and Earth, in *Solar Wind Eight*, edited by D. Winterhalter et al., *AIP Conf. Proc.*, *382*, 522.

Nakagawa, T., et al. (1989), Planar magnetic structures in the solar wind, *J. Geophys. Res.*, *94*, 11,761.
Neugebauer, M., et al. (1993), The origins of planar magnetic structures in the solar wind, *J. Geophys. Res.*, *98*, 9383.
Sanderson, T. R., et al. (2000), Effect of magnetic discontinuities on the propagation of energetic particles: Ulysses observations of the onset of the March 1991 solar particle event, *J. Geophys. Res.*, *105*, 18,275.
Tsurutani, B. T., et al. (1988), Origin of interplanetary southward magnetic fields responsible for major magnetic storms near solar maximum (1978–1979), *J. Geophys. Res.*, *93*, 8519.

R. Kataoka, K. Marubashi, N. Shimada, H. Shimazu, and S. Watari, National Institute of Information and Communications Technology, 4-2-1, Nukui-Kitamachi, Koganei, Tokyo, 184-8795, Japan. (ryuho@nict.go.jp)